PROCEEDINGS OF SCIENCE

The Gravitational Wave Transient Catalog 4.0: Overview and Highlights

Ofek Birnholtz[a,*] **on behalf of the LIGO-Virgo-KAGRA collaboration**

[a] *Bar-Ilan University,*
Max and Anna Webb Street, Ramat Gan, Israel

E-mail: ofek.birnholtz@biu.ac.il

The worldwide network of gravitational-wave (GW) detectors, comprised of the Advanced LIGO, Advanced Virgo, and KAGRA detectors, has been increasing in sensitivity, range, and hence quantity and quality of detected GW signals from compact binary coalescences. We present the compact binary signals observed and included in the GW Transient Catalog 4 (GWTC-4.0), i.e. up to and including the first part of the fourth observing run of the detectors (O4a). We estimate the source properties, and provide new insight into compact objects in binaries - and to what may lay ahead.

High Energy Astrophysics in Southern Africa (HEASA2025)
16-20 September, 2025
University of Johannesburg, South Africa

[1] Based on the presentation LIGO-G2501058
[*] Speaker

PoS(HEASA2025)011

Figure 1: Observatories in the gravitational wave network

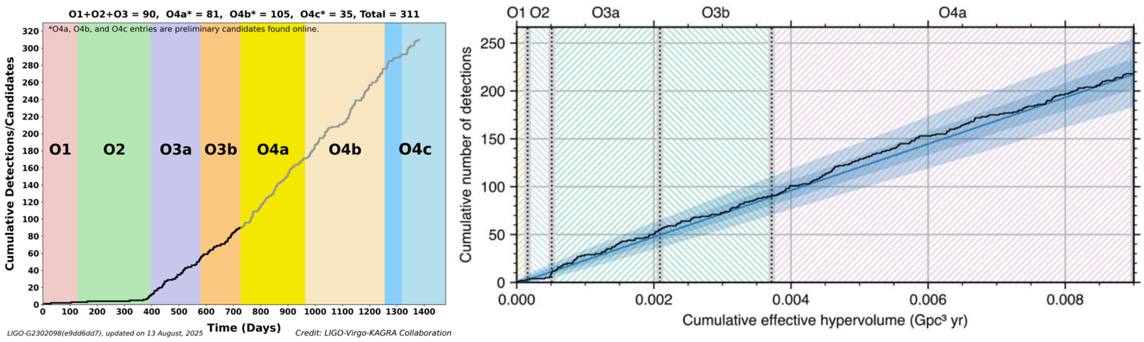

Figure 2: Left: GW events by observation times: O1-O3 numbers are published events; O4a-c count alerts issued. Right: GW events O1-O4a, by observed effective hypervolume (from [4]).

1. Introduction

This talk on behalf of the collaboration operating and supporting the gravitational wave (GW) detectors LIGO (Hanford and Livingston) [1], Virgo [2] and KAGRA [3] – the LVK (Fig. 1) – follows the announcement and release by the LVK of the fourth version of the gravitational wave transient catalog (GWTC-4.0) [4–14], in a special focus issue of ApJ Letters [15], and the opening of the relevant databases to the public [9–13, 16, 17]. The catalog includes GW detections ("events") from the first detection of the GW from the binary black hole (BBH) GW150914 [18] during the first observing run O1 [19], through the observing runs O2 [20], O3a [21] and O3b [22], and up to the first part of the fourth observing run (O4a). The O4a events are new, aside from two exceptional events which had been previously published, GW230529 [23, 24] and GW231123 [25]. The second part of the run (O4b) has also been completed, and at the time of this talk, the third part (O4c) is ongoing [26]. While the Virgo, KAGRA and GEO detectors contributed in previous runs, for O4a events only LIGO detectors' data were used. An additional LIGO detector, LIGO-Aundha, is under construction in India. This set of papers bears the names of about 1,800 authors from about 320 institutions, across 30 countries on 6 continents, and could not have been completed without great efforts.

Fig. 2 shows the progress of GW detections throughout the observing runs. On the left, the numbers given for O1-O3 are the published events from GWTC-1,2,3, while the O4 numbers indicate online alerts issued in low-latency. The slopes visibly change between runs. On the right, rate changes are shown to be consistent with the sensitive Time-Volume (hypervolume), according

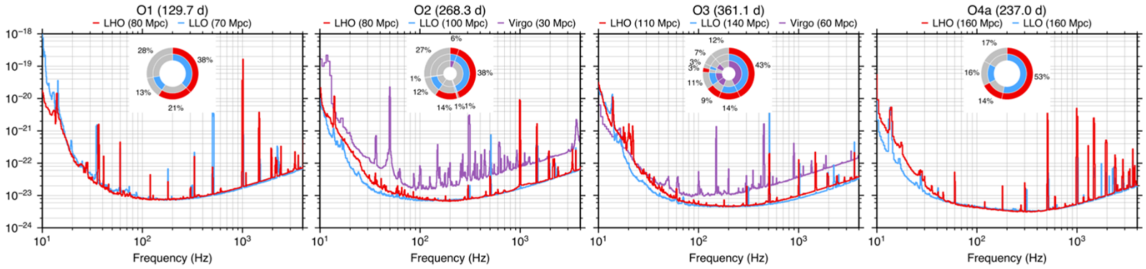

Figure 3: Noise Curves and Detector Network Duty Cycles, O1-O4a (from [4]).

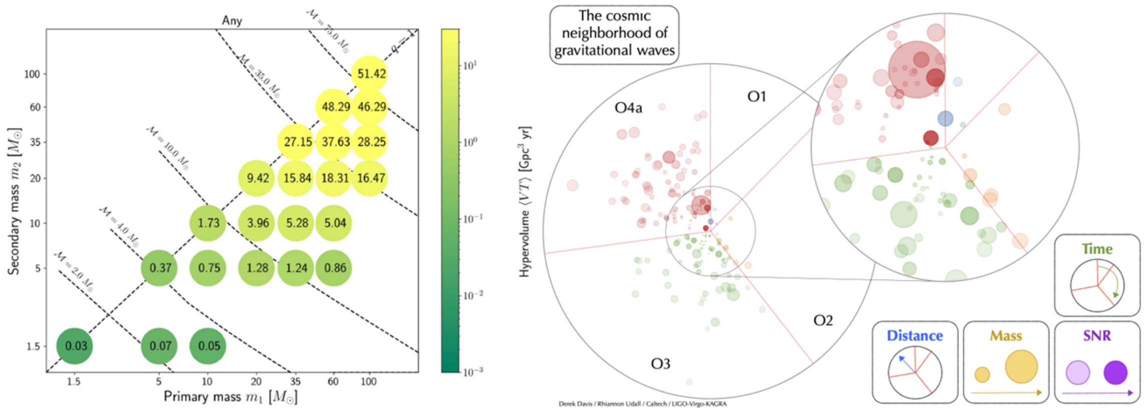

Figure 4: The GW detectors' Reach (from [6]).

to the reduction in detector noise, hence increase in detection range. The evolution of thoe noise curves is shown in Fig. 3. The ranges indicated are for the limit for detections of a $1.4M_\odot + 1.4M_\odot$ binary neutron star (BNS) system. The insets show the up-time and duty-cycles of the individual detectors and of the network, integrated and compactified over the run fragments. It thus shows the network combinations, for concurrent runtimes of LIGO Hanford (LHO), LIGO Livingston (LLO), and Virgo. KAGRA and GEO are not shown, as their ranges have been low. The effective range for detecting heavier systems, with different effective spins, in shown in Fig. 4.

The final number of events added in the O4a run, with a probability of astrophysical origin $p_{\rm astro} \geq 0.5$, is 128. Of these, the 86 with a false alarm rate FAR $< 1{\rm yr}^{-1}$ have been analyzed in Parameter Estimation pipelines [5, 6]. Thus there are a total of 218 events in GWTC-4.0. These are shown in Fig. 5. There is clearly a relative abundance of heavier mass systems, which can be detected much further, as is explained below.

2. Modeling

2.1 Basic

In General Relativity (GR) GWs are generated by the relativistically fast motion of massive systems [27–29]. When a system is only mildly relativistic, the GW can be calculated with Einstein's Quadrupole Formula, which gives the strain h_{ij} in terms of the time-varying quadrupole moment

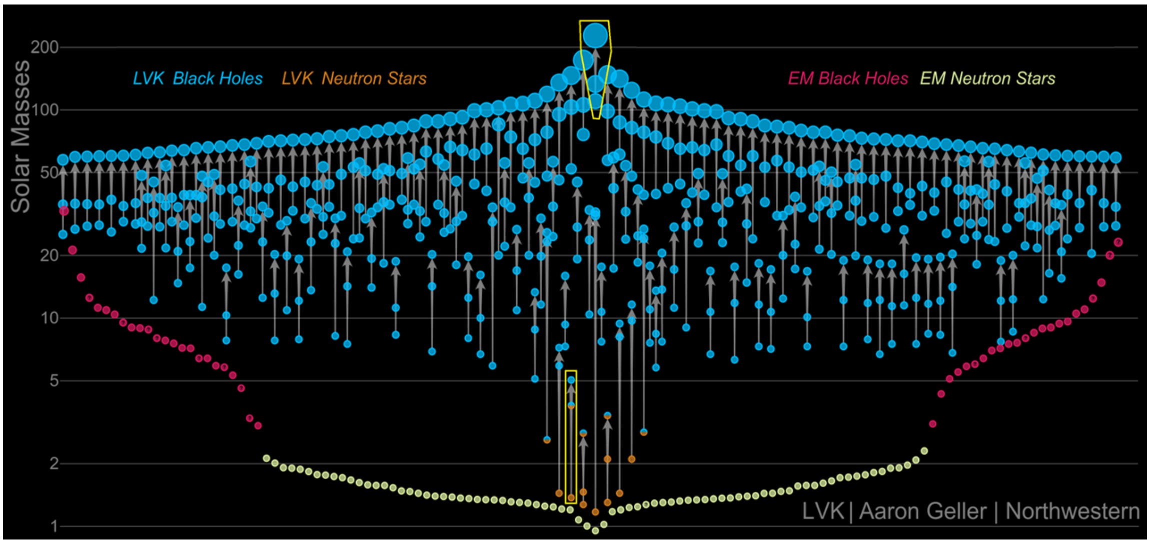

Figure 5: All GW events in GWTC-4.0. The vertical axis indicates mass in $M_\odot$; the horizontal is arbitrary. The exceptional events GW230529 and GW231123 are highlighted.

Q_{ij},

$$h_{ij} = \frac{2G}{c^4 d_L}\frac{d^2 Q_{ij}}{dt^2} \quad , \quad Q_{ij} = \int d^3x \rho(\mathbf{x}) \left(x_i x_j - \frac{1}{3} r^2 \delta_{ij} \right), \tag{1}$$

and the power output from the system is

$$\frac{dE_{GW}}{dt} = \frac{c^3}{16\pi G} \iint |\dot{h}| dS = \frac{1}{5}\frac{G}{c^5} \sum_{i,j=1}^{3} \frac{d^3 Q_{ij}}{dt^3}\frac{d^3 Q_{ij}}{dt^3}. \tag{2}$$

A binary system on a circular Newtonian orbit (an approximation valid in the infinite past) would thus lose energy to the emitted GWs, and thus sink to a lower orbit, i.e. "inspirals". Extracting this power adiabatically from the binary's mechanical energy, we can solve for the binary's orbital frequency evolution over time, hence for the GW's frequency over time (which is double the orbital), and find [27–29] that the evolution of f depends on a particular mass combination, the "chirp mass" $\mathcal{M}$,

$$\dot{f} = \frac{96}{5}\pi^{8/3}\left(\frac{G\mathcal{M}}{c^3}\right)^{5/3} f^{11/3} \quad , \quad \mathcal{M} = \frac{(m_1 m_2)^{3/5}}{(m_1+m_2)^{1/5}}. \tag{3}$$

As the detector has a limited window of frequencies where it is sensitive, $\dot{f}$ can be inverted and integrated from the frequency f_{ref} where it enters the window, to find the total time a signal spends within the window, as

$$\tau_0 = \frac{5}{256}(\pi f_{ref})^{-8/3}\left(\frac{G\mathcal{M}}{c^3}\right)^{-5/3}. \tag{4}$$

Using this, and the quadrupole formula, we can estimate the peak strain, luminosity range d_L, and hence sensitive volume V as

$$h \sim \frac{\mathcal{M}}{r} \quad , \quad d_L \propto \mathcal{M}^{5/6} \quad , \quad V \propto \mathcal{M}^{5/2}. \tag{5}$$

These explain the strong bias towards detecting high mass systems, as seen in Figs. 4 & 5.

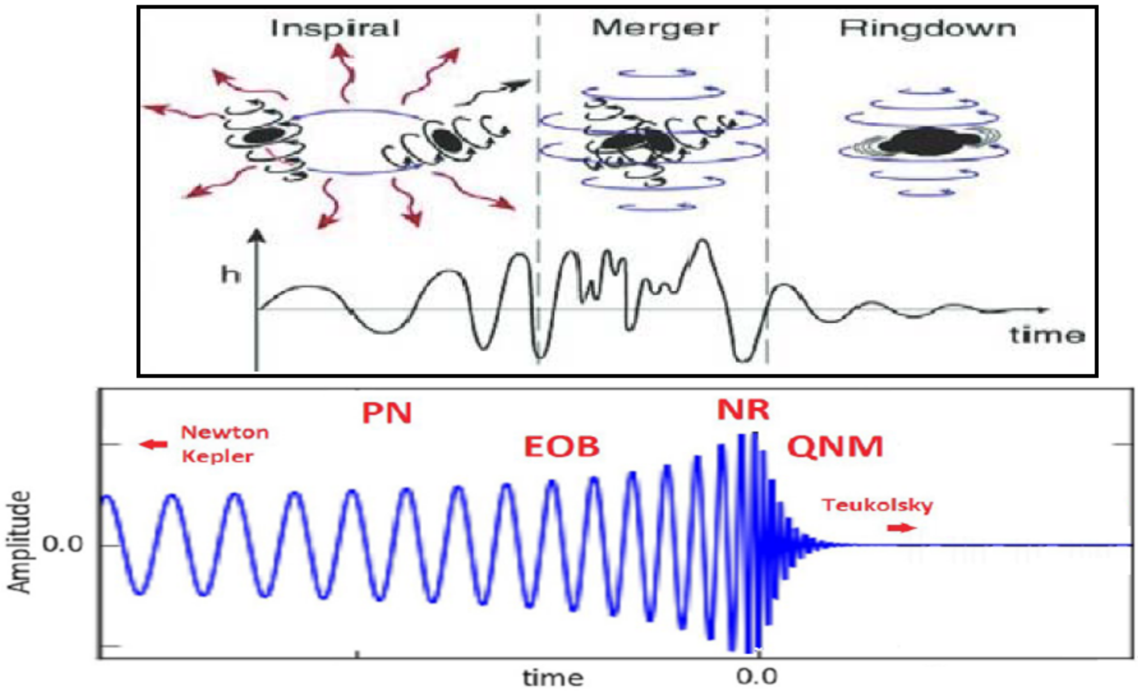

Figure 6: Top: Thorne's Cartoon (1999) on the IMR stages [30], before full numerical relativity waveforms. Bottom: Full GW waveform, produced by the author using the same IMR model as in [18] (2016).

2.2 Full Inspiral-Merger-Ringdown (IMR)

The Newtonian-Keplerian approximation of the inspiral is formally only correct in the infinite past; however, post-Newtonian (PN) [28, 29, 31] modifications enter in a slow and controllable fashion, in perturbations quantified by orders of the PN parameter $x \sim \left(\frac{v}{c}\right)^2 \sim \sqrt[3]{\pi G(m_1+m_2) f_{GW}}/c$, which have been calculated order by order for almost a century [32]. As x grows, the PN series fail to converge due to the underlying no-flatness of the spacetime; at which stage, an alternate model based on the curvature around an Effective One Body (EOB) [33] describes the system and the emerging GWs better.

On the other hand, late enough after two BHs have merged, the resulting spacetime should be similar enough to a single Kerr BH, perturbed. These perturbations are described by Teukolsky's equation [34], and have well-known quasinormal modes [35, 36], by which the spacetime "rings down" to a stationary steady Kerr BH.

These pair of early and late stages, the inspiral and the ringdown, had thus been understood analytically, and captured in Kip Thorne's cartoon [30], reproduced in the top of Fig. 6. The middle, however, representing the merger stage, had been expected to manifest the nonlinearities of GR, and lie beyond analytic treatment. However, the breakthrough in numerical relativity (NR) two decades ago [37, 38, 38–41] showed the merger to connect the inspiral to the merger in a regular fashion, as shown in the bottom of Fig. 6. This breakthrough enabled the development of waveform models covering the entire inspiral-merger-ringdown (IMR) regime, and templates of these types have been the basis for the LVK's matched filtering based searches for events [5, 10] and analysis,

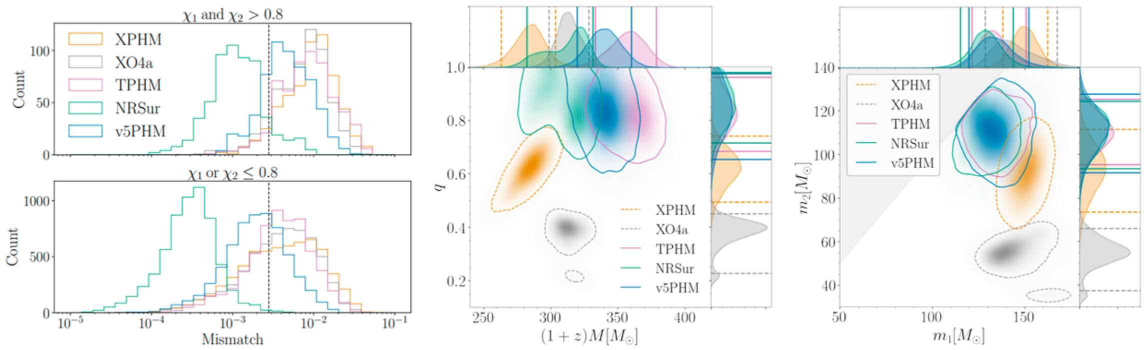

Figure 7: Parameter Estimation for GW231123 using different waveform models, and their discrepancies

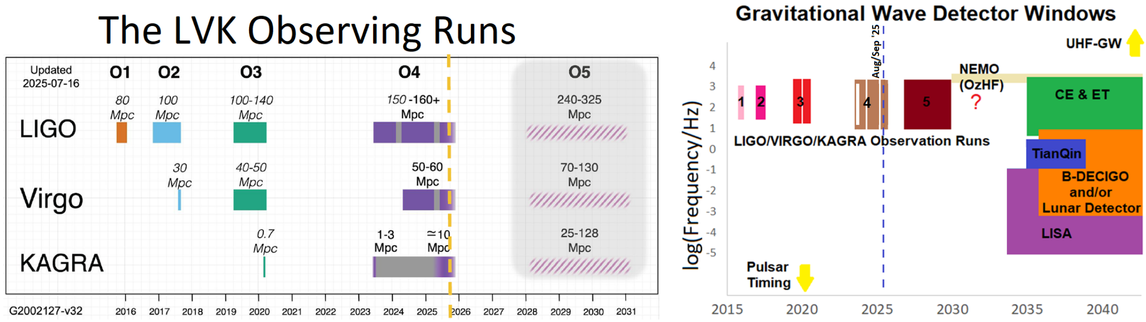

Figure 8: Left: Timeline of the LVK detector network through its past, present and future observing runs. Right: Timeline of detectors and coverage of the GW frequency spectrum

through parameter estimation, of the events found [5, 13].

This paper cannot begin to accommodate the breadth of these waveform models [5]; thus the only ones mentioned are those used for the analysis of GW231123 [25], as in Fig. 7: the top 3 are of the Inspiral-Merger-Ringdown Phenomenological (IMRPhenom) family, specifically: IMRPhenomXPHM [42], IMRPhenomXO4a [43], IMRPhenomTPHM [44] NRSur means Numerical Relativity Surrogate, specifically NRSur7dq4 [45] v5PHM refers to the Effective-One-Body (EOB) family, specifically SEOBNRv5PHM [46]. The additional acronyms include HM for Higher Modes, P for Processing, and T for Time Domain.

Fig. 7 further shows that different waveform models - even of the same family - do not always agree when estimating the parameters of the GW231123 (SNR~20) system [25]. Likewise, systematic differences between different waveform models have appeared for GWG230814 (SNR~42) [14]. These suggest that some waveform models, originally designed for searches of signals with modest (~ 10) SNR, and thus defined with a mismatch target of 3%, have systematic inaccuracies that manifest above the noise level for SNRs of a few 10's. This poses a challenge for the next generation of waveform models, as detectors increase in sensitivity and in numbers - even before the age of space detectors like LISA and 3rd generation terrestrial detectors like the Einstein Telescope (ET) and Cosmic Explorer (ET) (see Fig. 8).

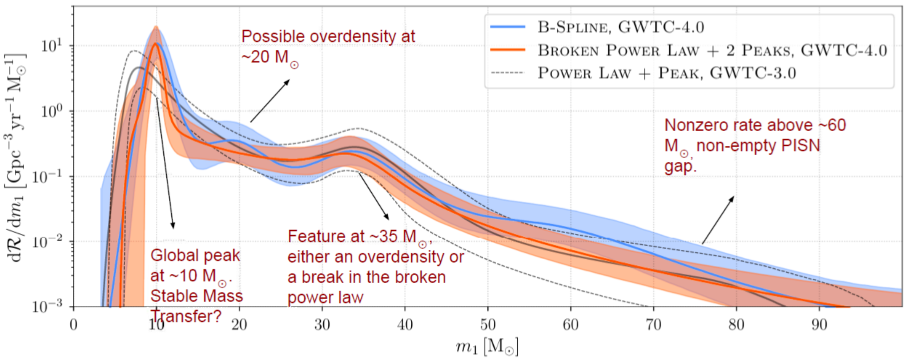

Figure 9: The mass distribution of the primary progenitors (from [7])

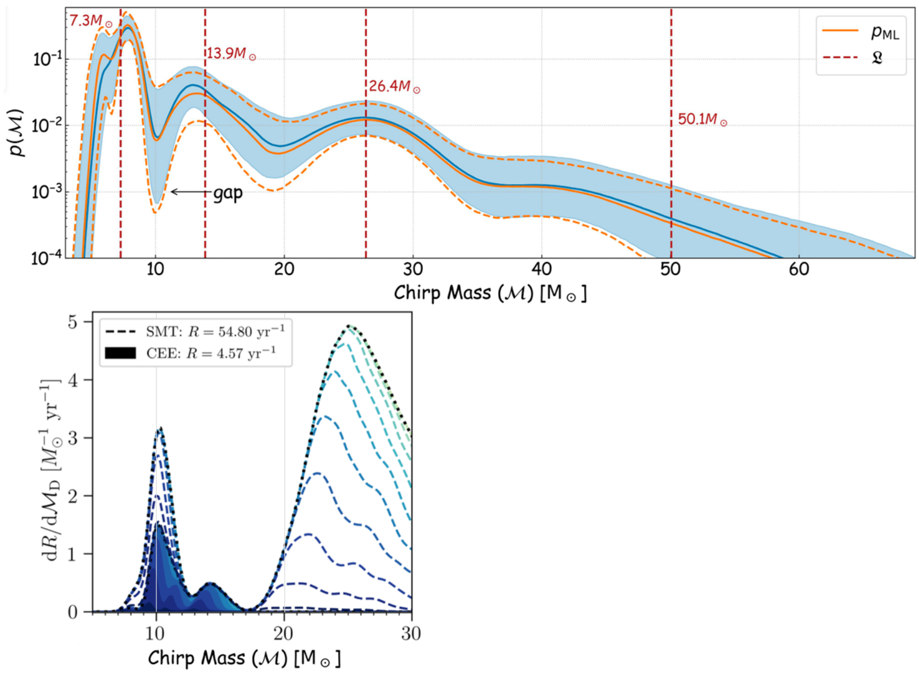

Figure 10: Top: The mass distribution of the chirp mass [47]. Bottom: a prediction for that distribution from binary stellar evolution [48], showing the peak between $20M_{\odot}$ to $30M_{\odot}$ lines up (other features do not).

3. Population - and the Future

In addition to studying individual GW events, the population and distributions of masses and parameters is already impacting and testing astrophysical stellar evolutionary models, especially for binaries, either in field or evolving together. The mass distribution of the GWTC-4.0 population is quoted here with two parameterizations: by the mass of the heavier progenitor (Fig. 9, from [7]) and by the chirp mass $\mathcal{M}$ (Top of Fig. 10, from [47]). The bottom of Fig. 10, with the axes aligned to the top, appears a prediction [48] based on binary stellar evolution. The relative peak around $26M_{\odot}$ is recovered, while features below $15M_{\odot}$ – less so.

Fig. 8 shows the plan for the next long LVK observing run, O5, as well as the plans for constructing more detectors, both more sensitive terrestrial detectors for the same frequency window, such as ET and CE, and new detectors, primarily in space, for looking at signals starting from (and even ending at) much lower frequencies. Other technologies promise to expand the GW spectrum even wider.

Acknowledgements

This material is based upon work supported by NSF's LIGO Laboratory which is a major facility fully funded by the (USA's) National Science Foundation.

References

[1] LIGO Scientific Collaboration collaboration, *Advanced LIGO*, *Class. Quantum Grav.* **32** (2015) 074001 [1411.4547].

[2] Virgo Collaboration collaboration, *Advanced Virgo: a second-generation interferometric gravitational wave detector*, *Class. Quantum Grav.* **32** (2015) 024001 [1408.3978].

[3] KAGRA collaboration, *Construction of KAGRA: an Underground Gravitational Wave Observatory*, *PTEP* **2018** (2018) 013F01 [1712.00148].

[4] LIGO Scientific, Virgo, KAGRA collaboration, *GWTC-4.0: An Introduction to Version 4.0 of the Gravitational Wave Transient Catalog*, 2508.18080.

[5] LIGO Scientific, Virgo, KAGRA collaboration, *GWTC-4.0: Methods for Identifying and Characterizing Gravitational-wave Transients*, 2508.18081.

[6] LIGO Scientific, Virgo, KAGRA collaboration, *GWTC-4.0: Updating the Gravitational-Wave Transient Catalog with Observations from the First Part of the Fourth LIGO-Virgo-KAGRA Observing Run*, 2508.18082.

[7] LIGO Scientific, Virgo, KAGRA collaboration, *GWTC-4.0: Population Properties of Merging Compact Binaries*, 2508.18083.

[8] LIGO Scientific, Virgo, KAGRA collaboration, *GWTC-4.0: Constraints on the Cosmic Expansion Rate and Modified Gravitational-wave Propagation*, 2509.04348.

[9] LIGO Scientific, Virgo, KAGRA collaboration, *Open Data from LIGO, Virgo, and KAGRA through the first part of the fourth observing run*, 2508.18079.

[10] LIGO Scientific, VIRGO, Kagra collaboration, *GWTC-4.0: Candidate Data Release*, 2025. 10.5281/zenodo.16053640.

[11] LIGO Scientific, VIRGO, Kagra collaboration, *GWTC-4.0: Glitch Modelling for Events*, 2025. 10.5281/zenodo.16857060.

[12] LIGO Scientific, VIRGO, Kagra collaboration, *GWTC-4.0: Data Quality Products for Transient Gravitational Wave Searches*, 2025. 10.5281/zenodo.16856919.

[13] LIGO Scientific, VIRGO, Kagra collaboration, *GWTC-4.0: Parameter Estimation Data Release*, 2025. 10.5281/zenodo.16053483.

[14] LIGO Scientific, VIRGO, Kagra collaboration, *GW230814: investigation of a loud gravitational-wave signal observed with a single detector*, 2509.07348.

[15] LIGO Scientific, Virgo, KAGRA collaboration, "Focus Issue on Version 4.0 of the Gravitational Wave Transient Catalog." 2025.

[16] LIGO Scientific, VIRGO, Kagra collaboration, *GWTC-4.0: O4a Search Sensitivity Estimates*, Aug., 2025. 10.5281/zenodo.16740117.

[17] LIGO Scientific, VIRGO, Kagra collaboration, *GWTC-4.0: Cumulative Search Sensitivity Estimates*, Aug., 2025. 10.5281/zenodo.16740128.

[18] LIGO Scientific Collaboration, Virgo Collaboration collaboration, *Observation of Gravitational Waves from a Binary Black Hole Merger*, Phys. Rev. Lett. **116** (2016) 061102 [1602.03837].

[19] LIGO Scientific, VIRGO collaboration, *Binary Black Hole Mergers in the first Advanced LIGO Observing Run*, Phys. Rev. X **6** (2016) 041015 [1606.04856].

[20] LIGO Scientific Collaboration, Virgo Collaboration collaboration, *GWTC-1: A Gravitational-Wave Transient Catalog of Compact Binary Mergers Observed by LIGO and Virgo during the First and Second Observing Runs*, Phys. Rev. X **9** (2019) 031040 [1811.12907].

[21] LIGO Scientific, Virgo collaboration, *GWTC-2: Compact Binary Coalescences Observed by LIGO and Virgo During the First Half of the Third Observing Run*, Phys. Rev. X **11** (2021) 021053 [2010.14527].

[22] KAGRA, VIRGO, LIGO Scientific collaboration, *GWTC-3: Compact Binary Coalescences Observed by LIGO and Virgo during the Second Part of the Third Observing Run*, Phys. Rev. X **13** (2023) 041039 [2111.03606].

[23] LIGO Scientific, KAGRA, VIRGO collaboration, *Observation of Gravitational Waves from the Coalescence of a 2.5–4.5 M Compact Object and a Neutron Star*, Astrophys. J. Lett. **970** (2024) L34 [2404.04248].

[24] E.M. Sänger et al., *Tests of General Relativity with GW230529: a neutron star merging with a lower mass-gap compact object*, 2406.03568.

[25] LIGO Scientific, VIRGO, KAGRA collaboration, *GW231123: A Binary Black Hole Merger with Total Mass 190–265 M*, Astrophys. J. Lett. **993** (2025) L25 [2507.08219].

[26] The LIGO Scientific Collaboration and the Virgo Collaboration and the KAGRA Collaboration, *Observing Scenario timeline graphic, post-O3*, Tech. Rep. LIGO-P1200087, The LIGO Scientific Collaboration and the Virgo Collaboration and the KAGRA Collaboration (2020).

[27] B.F. Schutz, *GRAVITATIONAL WAVES ON THE BACK OF AN ENVELOPE*, *Am. J. Phys.* **52** (1984) 412.

[28] M. Maggiore, *Gravitational wave experiments and early universe cosmology*, *Phys.Rept.* **331** (2000) 283 [gr-qc/9909001].

[29] LIGO Scientific, Virgo collaboration, *The basic physics of the binary black hole merger GW150914*, *Annalen Phys.* **529** (2017) 1600209 [1608.01940].

[30] K. Thorne, *Spacetime warps and the quantum : A glimpse of the future*, in *The Future of Spacetime*, R.H. Price, ed., pp. 109–152, W.W. Norton, New York (2002), https://www.cco.caltech.edu/ kip/index.html/PubScans/VI-42.pdf.

[31] L. Blanchet, *Gravitational radiation from post-Newtonian sources and inspiralling compact binaries*, *Living Rev. Rel.* **17** (2014) 2 [gr-qc/0202016].

[32] A. Einstein, L. Infeld and B. Hoffmann, *The Gravitational Equations and the Problem of Motion*, *Annals of Mathematics* **39** (1938) 65.

[33] A. Buonanno and T. Damour, *Effective one-body approach to general relativistic two-body dynamics*, *Phys. Rev. D* **59** (1999) 084006 [gr-qc/9811091].

[34] S.A. Teukolsky, *Perturbations of a rotating black hole. 1. Fundamental equations for gravitational electromagnetic and neutrino field perturbations*, *Astrophys. J.* **185** (1973) 635.

[35] E. Berti, V. Cardoso and C.M. Will, *On gravitational-wave spectroscopy of massive black holes with the space interferometer LISA*, *Phys. Rev. D* **73** (2006) 064030 [gr-qc/0512160].

[36] E. Berti, V. Cardoso and A.O. Starinets, *Quasinormal modes of black holes and black branes*, *Class. Quantum Grav.* **26** (2009) 163001 [0905.2975].

[37] F. Pretorius, *Evolution of binary black hole spacetimes*, *Phys. Rev. Lett.* **95** (2005) 121101 [gr-qc/0507014].

[38] J.G. Baker, M. Campanelli, C.O. Lousto and R. Takahashi, *Modeling gravitational radiation from coalescing binary black holes*, *Phys. Rev. D* **65** (2002) 124012 [astro-ph/0202469].

[39] A. Buonanno, G.B. Cook and F. Pretorius, *Inspiral, merger and ring-down of equal-mass black-hole binaries*, *Phys. Rev. D* **75** (2007) 124018 [gr-qc/0610122].

[40] J.G. Baker, J. Centrella, D.-I. Choi, M. Koppitz and J. van Meter, *Gravitational wave extraction from an inspiraling configuration of merging black holes*, *Phys. Rev. Lett.* **96** (2006) 111102 [gr-qc/0511103].

[41] J.G. Baker, M. Campanelli, F. Pretorius and Y. Zlochower, *Comparisons of binary black hole merger waveforms*, Class. Quant. Grav. **24** (2007) S25 [gr-qc/0701016].

[42] M. Colleoni, F.A.R. Vidal, C. García-Quirós, S. Akçay and S. Bera, *Fast frequency-domain gravitational waveforms for precessing binaries with a new twist*, Phys. Rev. D **111** (2025) 104019 [2412.16721].

[43] J.E. Thompson, E. Hamilton, L. London, S. Ghosh, P. Kolitsidou, C. Hoy et al., *PhenomXO4a: a phenomenological gravitational-wave model for precessing black-hole binaries with higher multipoles and asymmetries*, Phys. Rev. D **109** (2024) 063012 [2312.10025].

[44] H. Estellés, M. Colleoni, C. García-Quirós, S. Husa, D. Keitel, M. Mateu-Lucena et al., *New twists in compact binary waveform modeling: A fast time-domain model for precession*, Phys. Rev. D **105** (2022) 084040 [2105.05872].

[45] V. Varma, S.E. Field, M.A. Scheel, J. Blackman, D. Gerosa, L.C. Stein et al., *Surrogate models for precessing binary black hole simulations with unequal masses*, Phys. Rev. Research. **1** (2019) 033015 [1905.09300].

[46] A. Ramos-Buades, A. Buonanno, H. Estellés, M. Khalil, D.P. Mihaylov, S. Ossokine et al., *Next generation of accurate and efficient multipolar precessing-spin effective-one-body waveforms for binary black holes*, Phys. Rev. D **108** (2023) 124037 [2303.18046].

[47] V. Tiwari, *Population of Binary Black Holes Inferred from One Hundred and Fifty Gravitational Wave Signals*, 2510.25579.

[48] Willcox and Podiaslowski, *private communication*, 08, 2025.